

## Original Article

# ICOSL expressed in triple-negative breast cancer can induce Foxp3+ Treg cell differentiation and reverse p38 pathway activation

Ning Ma<sup>1\*</sup>, Tianran Chen<sup>2\*</sup>, Yingyi Zhang<sup>2\*</sup>, Longpei Chen<sup>2</sup>, Jie Li<sup>2</sup>, Xiaobo Peng<sup>2</sup>, Yajie Wang<sup>2</sup>, Dongxun Zhou<sup>3</sup>, Bin Wang<sup>2</sup>

<sup>1</sup>Department of Clinical Laboratory, 905th Hospital of PLA, Naval Medical University, 1328 Huashan Road, Shanghai 200050, P. R. China; <sup>2</sup>Department of Oncology, Changhai Hospital, Naval Medical University, 168 Changhai Road, Shanghai 200433, P. R. China; <sup>3</sup>Department of Endoscopy and Gastroenterology, Eastern Hepatobiliary Hospital, Naval Medical University, 225 Changhai Road, Shanghai 200433, P. R. China. \*Equal contributors.

Received June 30, 2022; Accepted August 9, 2022; Epub September 15, 2022; Published September 30, 2022

**Abstract:** Inducible costimulator ligand (ICOSL) expressed on cancer cells has immunoregulatory functions in various malignancies. However, the role of ICOSL in triple-negative breast cancer (TNBC) remains unclear. In this study, the role and expression of ICOSL in TNBC were analyzed using the cBioPortal and GEPIA databases. Then the role of ICOSL in Foxp3+ Treg cell differentiation, reversal of p38 pathway activation and cell proliferation, migration and apoptosis was determined in vitro. Finally, the effect of ICOSL expression on TNBC progression was verified in a nude mouse model of TNBC. We here observed that ICOSL expression in TNBC was found to be related to relapse-free survival, and Treg abundance was positively correlated with ICOSL expression, as demonstrated by database analyses. In vitro experiments showed that ICOSL overexpression (OE) in MDA-MB-231 cells induced cocultured T cells to differentiate into Foxp3+ Treg cells and promoted secretion of the tumor-promoting factors IL-10 and IL-4. Furthermore, in vitro experiments showed that ICOSL reversed p38 phosphorylation and promoted the proliferation, invasion, and metastasis of MDA-MB-231 ICOSL-OE cells. Finally, tumor progression was found to be promoted by ICOSL expression in a TNBC nude mouse model. Together, ICOSL expression can enhance tumor cell growth by inducing Foxp3+ Treg cell differentiation and reversing p38 pathway activation in TNBC.

**Keywords:** ICOSL, triple-negative breast cancer, Foxp3, Treg

## Introduction

The incidence of female breast cancer ranks first in the incidence of malignant tumors in women in China [1, 2]. Triple-negative breast cancer (TNBC) is one of the breast cancer types with the worst prognosis [3-5]. It occurs earlier and metastasizes more easily than other types of breast cancer [6]. Once breast cancer metastasizes, the median overall survival is only 2-3 years [6]. In recent years, significant progress has been made in immunotherapy for breast cancer treatment. An increasing number of studies have focused on TNBC, which has a high number of tumor-infiltrating lymphocytes (TILs) [7-10]. Therefore, it is important to explore how TNBC cells evade immune surveillance by regulating immune reactivity.

T-cell receptor (TCR) recognition antigen (Ag) and major histocompatibility complex (MHC) are necessary prerequisites for T-cell activation signal 1 [11]. However, Ag-independent signaling through costimulatory receptors is also necessary as signal 2 to complete the activation of naive T cells. The second step requires CD28 to interact with one of its ligands (B7-1 or B7-2) on antigen-presenting cells (APCs) [12]. Inducible costimulator (ICOS) is a member of the B7 family and is expressed only on activated T cells. ICOS ligand (ICOSL) may be found in APCs, such as B lymphocytes, dendritic cells, and some cancer cells (e.g., gastric carcinoma cells) [13]. ICOSL is a positive costimulatory molecule that stimulates type 2 T helper (Th2) and regulatory T (Treg) cell responses but not Th1 cell responses [14].

# ICOSL enhances tumor progression in TNBC

Currently, it is not clear how ICOSL expressed on tumor cells mediates the immune response and participates in the occurrence and development of tumors. Some experiments have shown that ICOSL is associated with a poor prognosis in acute myeloid leukemia cells, and other studies have suggested that ICOSL contributes to tumor regression in solid tumors [15]. Our group collected 562 invasive breast cancer tumor specimens to explore the role of ICOSL in breast cancer. We found that upregulation of ICOSL was associated with worse prognosis in Chinese patients with breast cancer [16]. Our colleagues, Tang et al., found that ICOSlg and ICOSL interaction on mouse bone marrow-derived dendritic cells (DCs) not only induces a p38-MAPK-dependent elevation of interleukin 6 (IL-6) but also enhances phagocytosis and the antigen-presentation function of DCs in vitro, indicating that ICOS can deliver reverse signals to ICOSL-expressing cells through the ICOSlg-ICOSL interaction [17].

To date, neither the role of T-cell induction and activation by ICOSL expressed on TNBC tumor cells nor the effect on the reverse signals on tumor cells have been reported. Based on our previous studies, our research further demonstrated the important role of ICOSL in inducing Treg cell differentiation and reversing p38 pathway activation in TNBC.

## Materials and methods

### *Database analysis*

#### *Dataset collection and preprocessing*

Gene expression profiles and the corresponding clinical information were downloaded from cBioPortal ([www.cbioportal.org](http://www.cbioportal.org)). Patients with breast invasive lobular carcinoma of no special type and patients with breast invasive ductal carcinoma were selected to build the breast cancer dataset. We divided the TNBC dataset from the breast cancer dataset, where estrogen receptor (ER), human epidermal growth factor receptor 2 (HER2), and progesterone receptor (PR) statuses were labeled negative. The remainder was grouped into the non-TNBC dataset. Patients in the TNBC and non-TNBC datasets were classified into high and low ICOSL expression groups.

### *Analysis of clinical characteristics*

Fisher's exact test and logistic regression were applied to evaluate the distribution of clinical characteristics in the TNBC and non-TNBC groups. To reveal the roles of clinical features in patient overall survival and tumor relapse, univariate Cox analysis and prognostic nomogram models were constructed based on selected clinical features. Kaplan-Meier survival analysis was performed to illustrate the influence of triple-negative status or ICOSL expression on patient survival or tumor relapse.

### *GEPIA and protein atlas database analysis*

The GEPIA database (<http://gepia.cancer-pku.cn/>) was used to explore the ICOSL expression levels in normal and breast cancer samples [18]. We retrieved the ICOSL immunohistochemistry (IHC) data of normal breast tissue and breast cancer tissue from the Human Protein Atlas database (<http://www.proteinatlas.org/>).

### *Identification of differentially expressed genes (DEGs)*

The "limma" package in R was used to screen DEGs, with parameters of  $|\log_2\text{-fold change}| > 0.3$  and  $P < 0.05$  [19].

### *Enrichment analysis and functional annotation*

The "ClusterProfiler" package in R was used to conduct functional annotations, KEGG pathway enrichment, and gene set enrichment analysis (GSEA) [20].

### *Evaluation of immune cell infiltration*

Immune cell abundance was estimated using "CIBERSORT" in R. The CIBERSORT algorithm calculates the proportion of cells from the bulk tissue gene expression profiles [21].

### *Protein-protein interaction network analysis and identification of hub genes*

The DEGs were submitted to STRING online tools (<https://string-db.org/>) to establish a protein-protein interaction (PPI) network [22]. The molecular complex detection (MCODE) [23] plugin in Cytoscape [24] was used to explore the densely connected regions, and genes in

## ICOSL enhances tumor progression in TNBC

densely connected regions were regarded as hub genes.

### *Experiments*

#### Cell lines

MDA-MB-231 (human breast cancer cell line), WM35 (human melanoma cell line) and H9 (human T lymphocyte line) cells were obtained from the Cell Bank of Type Culture Collection, Shanghai Institute of Cell Biology, Chinese Academy of Sciences (Shanghai, China). The tumor cell lines were grown in culture dishes in RPMI 1640 medium plus 10% fetal bovine serum (FBS) (Life Technologies, Carlsbad, California, USA), 100 U/mL penicillin, and 100 µg/mL streptomycin at 37°C in a humidified atmosphere with 5% CO<sub>2</sub>.

#### Animals

Adult female nude mice were obtained from Changzhou Cavins Experimental Animal Co., Ltd. (Changzhou, China). The mice used in this study were 6-8 weeks of age. The mice were housed in sterilized microisolator cages and received normal chow and autoclaved drinking water. They were maintained under standard conditions and cared for according to the Second Military Medical University guidelines for animal care. All animal experiments were approved by the Committee on the Use of Live Animals in Teaching and Research.

#### ICOSL/ICOS overexpression in MDA-MB-231/H9 cells

Sequence fragments were synthesized according to the gene and vector sequences in the NCBI database. The ICOSL (Gene ID: 50723) and ICOS (Gene ID: 29851) genes were recombined and cloned into the pEZ-Lv201 lentivirus vector using the Gateway system.

Overexpression vectors were constructed and sequenced to identify successful construction. MDA-MB-231 and H9 cells were inoculated into 6-well plates at  $1 \times 10^5$ /well and infected with ICOSL/ICOS overexpression lentivirus (termed ICOSL-OE/ICOS-OE) or negative control lentivirus for 72 h. The RPMI 1640 medium plus 10% FBS was replaced, and fluorescence was observed to screen and obtain cell lines stably expressing ICOSL/ICOS. The specificity

and efficiency were validated by western blotting and quantitative reverse transcription polymerase chain reaction (qRT-PCR). ICOSL-negative MDA-MB-231 cells were further sorted from ICOSL-control lentivirus-infected MDA-MB-231 cells and used as MDA-MB-231 controls in all the subsequent experiments.

#### Western blot analysis

Total cell lysates were prepared and analyzed via SDS-PAGE, as previously described [25]. For quantification, the bands were measured using the Alphamager 2200 system (Alpha Innotech, San Leandro, CA) and normalized to β-actin levels. The expression levels of ICOS, ICOSL, p38, and p-p38 were quantified and are expressed as a ratio to GAPDH expression. The experiments were repeated three times using independent batches of cell clones or cell lysates. Quantitative data are presented as values relative to those of the control cells.

#### Cocultivation of MDA-MB-231 cells with CD4+ T cells

CD4+ T cells were collected from HLA-A0201 volunteers. Peripheral blood mononuclear cells (PBMCs) were isolated from 10 mL human blood in heparin sodium anticoagulant using the Ficoll-Hypaque method. Cells were suspended in 800 µL PBS with 200 µL anti-CD4-labeled magnetic microspheres (BD Biosciences, New Jersey, USA) and incubated at 4°C for 2 h. The proportion of CD4+ T cells was confirmed by flow cytometry. MDA-MB-231 cells in the logarithmic growth phase were treated with 1 mg/mL mitomycin for 1 h to inhibit growth. MDA-MB-231 cells ( $9 \times 10^6$  cells/mL) were cultured in 6-well plates with RPMI 1640 medium plus 10% fetal bovine serum. ICOSL antibody (10 µg/mL) was added to Group D. Four groups were prepared as follows: A. CD4+ T cells; B. CD4+ T cells + MDA-MB-231-control cells; C. CD4+ T cells + MDA-MB-231-ICOSL-OE cells; and D. CD4+ T cells + MDA-MB-231-ICOSL-OE cells + anti-ICOSL antibody. After 30 minutes of incubation, rIL-2 was added to each group at a concentration of 100 U/mL. Finally, CD4+ T cells were added. The final concentrations of MDA-MB-231 and CD4+ T cells were  $3 \times 10^6$ /mL and  $1 \times 10^6$ /mL, respectively. The total volume was 3 mL (MDA-MB-231:CD4+ T cells = 3:1). Groups A and B were used as negative con-

## ICOSL enhances tumor progression in TNBC

trols. The medium was changed every 12 h for 7 days. The cytokine levels were measured, and the rate of FOXP3<sup>+</sup>/ICOS<sup>+</sup> T cells among CD4<sup>+</sup> T cells was analyzed via flow cytometry.

### ELISA

After 7 days of cultivation, the supernatant was collected, and an ELISA kit (QuantiCyto, China) was used to detect the levels of TNF- $\alpha$ , IFN- $\gamma$ , IL-10, and IL-4 (QuantiCyto, China). Detection buffer (50  $\mu$ L) and prediluted samples (50  $\mu$ L) were added to sample wells. Two-fold diluted standard samples (100  $\mu$ L) were added to duplicate wells. Each well with the diluted detection antibody was incubated at room temperature for 1.5 h. After addition of the color-developing substrate, the results were read at OD 450 nm.

### Flow cytometry for analysis of ICOS/FOXP3<sup>+</sup> T cells

Approximately  $1 \times 10^6$  cells were counted and stained with the following monoclonal antibodies: FITC-anti-CD4, PE-anti-ICOS, APC-anti-ICOSL (BioLegend, USA), and human FoxP3 APC-conjugated antibody (R&D Systems, USA). Subsequently, the cells were washed, fixed, permeabilized with Cvtofix/Cytoperm buffer (BD Bioscience, USA) and then analyzed via flow cytometry as previously described [26].

### Cell counting kit-8 (CCK8) analysis

Martin-Orozco N et al. showed [27] that WM35 melanoma cells express high levels of ICOS-L. ICOS-L expression by melanoma tumor cells can directly drive Treg activation and expansion in the tumor microenvironment as another mechanism of immune evasion. Here, WM35 cells were also used in our study as a control to clarify the effect of ICOSL expressed on tumor cells when cultured with CD4<sup>+</sup> T cells. According to the above method, MDA-MB-231 ICOSL-OE cells or WM35 cells ( $3 \times 10^6$ /mL) were cultured with CD4<sup>+</sup> T cells ( $1 \times 10^6$ /mL) collected from volunteers. On Day 7, the tumor cells were isolated and cultured in 96-well plates. At 24, 48, and 72 h, the absorbance was measured at 450 nm to analyze the effect of ICOSL expression on tumor cell proliferation in TNBC using CCK8 assays (Beyotime, China) according to the protocol. The 6 groups were as follows: 1. MDA-MB-231 ICOSL-OE cells; 2. MDA-

MB-231 ICOSL-OE cells + CD4<sup>+</sup> T cells; 3. MDA-MB-231 ICOSL-OE cells + CD4<sup>+</sup> T cells + anti-ICOSL antibody; 4. WM35 cells; 5. WM35 cells + CD4<sup>+</sup> T cells; 6. WM35 cells + CD4<sup>+</sup> T cells + anti-ICOSL antibody.

### Cell apoptosis assays

Tumor cells were obtained after coculture with CD4<sup>+</sup> T cells as described in Section 2.2.8. MDA-MB-231-ICOSL-OE cells were inoculated into 6-well plates at a concentration of  $1 \times 10^5$ /mL with 2 mL/well and incubated at 37°C in a 5% CO<sub>2</sub> incubator for 24 h. Six groups were included as described in Section 2.2.8. The cells were harvested and rinsed twice with pre-cooled PBS. The samples were diluted with 150  $\mu$ L of 1 $\times$  annexin-binding buffer, and 5  $\mu$ L of APC-labeled enhanced annexin V and 5  $\mu$ L (20  $\mu$ g/mL) of propidium iodide (PI) were added. The cells were then incubated in the dark for 15 min at room temperature. Flow cytometry was conducted using a FACSCalibur instrument (Becton Dickinson, CA, USA).

### Phosphokinase array experiments

According to the above method, MDA-MB-231-ICOSL-OE cells ( $3 \times 10^6$ /mL) were cocultured with CD4<sup>+</sup> T cells ( $1 \times 10^6$ /mL) for 7 days to induce FOXP3<sup>+</sup> Treg cells. The CD4<sup>+</sup> T cells were collected and cocultured with MDA-MB-231-control or MDA-MB-231 ICOSL-OE cells. After incubation at 37°C for 48 h, the MDA-MB-231-control and MDA-MB-231-ICOSL-OE cells were collected and treated with fisetin and quercetin at a concentration of 200  $\mu$ M for 6 h, respectively. A human phospho-kinase dot blot array (ARY003B; R&D Systems) was used to simultaneously detect the relative phosphorylation levels of 43 human kinases and the total amounts of 2 related proteins. An equal amount of cell lysate (300  $\mu$ g) from each TNBC cell line was used for these experiments, as previously described [28].

### Analysis of the role of ICOSL in p38 phosphorylation, which can affect proliferation, apoptosis, migration, invasion, and cell cycle progression in MDA-MB-231 cells

To determine the role of ICOSL expression in p38 phosphorylation, MDA-MB-231-ICOSL-OE cells were inoculated into 6-well plates at a concentration of  $1 \times 10^5$ /mL with 2 mL/well; rhl-

## ICOSL enhances tumor progression in TNBC

COS-Fc and SB202190 were added at final concentrations of 5 µg/mL and 10 µmol/L, respectively. Sb202190 is a specific inhibitor of p38 α and p38 β through competition with ATP for the same binding site on p38. The protein expression levels of p38 and p-p38 were detected by western blotting. The groups were as follows: 1. MDA-MB-231-ICOSL-OH; 2. MDA-MB-231-Con + rhICOS-Fc; 3. MDA-MB-231-ICOSL-OH + rhICOS-Fc + SB202190.

After that, the tumor cells were incubated and cultured as described above. The groups were as follows: 1. MDA-MB-231-Con; 2. MDA-MB-231-Con + rhICOS-Fc; 3. MDA-MB-231-ICOSL-OE; 4. MDA-MB-231-ICOSL-OE + rhICOS-Fc; 5. MDA-MB-231-ICOSL-OE + rhICOS-Fc + SB202190. Rh-COS-Fc and SB202190 were added at final concentrations of 5 µg/mL and 10 µmol/L, respectively.

CCK8 assays and apoptosis analysis were performed according to the protocol mentioned above. The transwell migration assay and cell cycle analysis protocols were as follows.

*Transwell migration assay:* Cell migration was assayed using Transwells (BD Biosciences, USA) with PET track-etched membranes. Tumor cells were collected, adjusted to  $3 \times 10^5$ /mL and incubated in the upper chambers, and extra Matrigel was added for the migration assays. Medium containing 10% serum (800 µL) was added to the lower chambers, and the cells were incubated for 24 hours. The upper chamber was moved into a well with 800 µL methanol and 800 µL 0.2% crystal violet dye for 30 min. The migrated cells located on the lower surface of the upper chambers were counted three times in three random fields using a microscope.

*Cell cycle analysis via flow cytometry:* Breast cancer cells were seeded in 6-well culture plates and treated with decursin for 24 h. For cell cycle analysis, cells were harvested and fixed in 70% ice-cold ethanol overnight at -20°C. Cells were washed with PBS, and the samples were incubated with FxCycle™ propidium iodide/RNase Staining Solution (Invitrogen) for 30 min at room temperature. Cell cycle analysis was conducted according to the protocol for a CycleTEST™ PLUS DNA Reagent Kit, and data acquisition and analysis were

performed using a FACSCalibur flow cytometer (Becton Dickinson, CA).

### MDA-MB-231 breast cancer mouse model

Here, H9 cells (a human T lymphocyte line) were used as a tool cell to provide the receptor ICOS to activate the ligand ICOSL on tumor cells after overexpression of ICOS in H9 cells. H9 cells were inoculated into 6-well plates at  $1 \times 10^5$ /well and infected with ICOS overexpression lentivirus (termed ICOS-OE) or negative control lentivirus for 72 h as described above. Cells negative for ICOS-control lentivirus were sorted and used as an H9 control cell in a mouse model.

Adult female nude mice (6-8 weeks of age) were housed in sterilized microisolator cages and received normal chow and autoclaved hyperchlorinated drinking water. Briefly,  $1 \times 10^5$  MDA-MB-231 cells were inoculated into the right armpit of nude mice to construct a tumor model of TNBC. The mice were divided into 4 groups as follows: 1. MDA-MB-231-Con + H9-Con; 2. MDA-MB-231-Con + H9-ICOS-OE; 3. MDA-MB-231-ICOSL-OE + H9-Con; and 4. MDA-MB-231-ICOSL-OE + H9-ICOS-OE. The nude mice in Groups 1 and 3 were injected with  $1.0 \times 10^6$  H9-Con cells, and the nude mice in Groups 2 and 4 were injected with  $1.0 \times 10^6$  H9-ICOS-OE cells. Furthermore, the H9 cells in each group were treated with 40 µg/mL mitomycin for 30 min before injection. From Day 7 after the injection of MDA-MB-231 cells, the mice were closely monitored every 3 days and weighed, and the tumor volume was measured. The tumor volume was calculated as follows:  $\text{volume} = (\text{length} \times \text{width}^2)/2$ . Five weeks after tumor cell inoculation, in vivo imaging analysis was performed. The mice were sacrificed, and the tumors were excised. Each tumor was weighed, and the tumor volume was measured.

### Statistical analysis

SPSS (version 13.0, IBM, USA) was used for statistical analyses. The results are expressed as the mean ± standard deviation. The mean between two groups was compared using a grouped t test. Each experiment was repeated three times. Differences were considered statistically significant when the two-sided *P* value was less than 0.05.

# ICOSL enhances tumor progression in TNBC

**Table 1.** Breast cancer dataset characteristics

Characteristics	Level	Low ICOSL expression	High ICOSL expression	P	Test
Age	≤60	323 (40.5%)	387 (48.5%)	0.001	Exact
	>60	475 (59.5%)	411 (51.5%)		
Neoplasm histological grade	1	74 (9.6%)	34 (4.4%)	0.000	Exact
	2	354 (45.9%)	245 (31.9%)		
	3	343 (44.5%)	488 (63.6%)		
Chemotherapy	Yes	136 (17%)	223 (27.9%)	0.000	Exact
	No	662 (83%)	575 (72.1%)		
Hormone therapy	Yes	554 (69.4%)	436 (54.6%)	0.000	Exact
	No	244 (30.6%)	362 (45.4%)		
Breast surgery type	MASTECTOMY	474 (59.8%)	475 (60.6%)	0.797	Exact
	BREAST-CONSERVING	318 (40.2%)	309 (39.4%)		
Cellularity	High	401 (51.7%)	403 (51.8%)	1.000	Exact
	Moderate	295 (38.1%)	287 (36.9%)	0.637	Exact
	Low	79 (10.2%)	88 (11.3%)	0.513	Exact
Histologic subtype	Ductal/NST	721 (90.4%)	733 (91.9%)	0.333	Exact
	Lobular	77 (9.6%)	65 (8.1%)		
Inferred menopausal state	Pre	151 (18.9%)	204 (25.6%)	0.002	Exact
	Post	647 (81.1%)	594 (74.4%)		
Lymph nodes examined positive	0	423 (53%)	387 (48.5%)	0.080	Exact
	≥1	375 (47%)	411 (51.5%)		
Nottingham prognostic index	≤4	285 (35.7%)	199 (24.9%)	0.000	Exact
	>4	513 (64.3%)	599 (75.1%)		
TNBC	Yes	56 (7%)	212 (26.6%)	0.000	Exact
	No	742 (93%)	586 (73.4%)		

## Results

*TNBC was significantly associated with ICOSL expression, as demonstrated by database analysis*

Gene expression profiles and corresponding clinical information were downloaded from cBioPortal ([www.cbioportal.org](http://www.cbioportal.org)). As shown in **Table 1**, in the breast cancer dataset, ICOSL expression was correlated with many clinical features, including age, neoplasm histological grade, chemotherapy, hormone therapy, inferred menopausal state, Nottingham prognostic index, and TNBC.

ICOSL expression was analyzed in breast cancer (TCGA) and healthy individuals (GTEx) using the GEPIA database and evaluated in breast cancer (**Figure 1A**). Furthermore, among patients with breast cancer, TNBC patients tended to have higher expression levels than non-TNBC patients (**Figure 1B**). Furthermore, ICOSL

expression in all breast cancer cases in TCGA was significantly correlated with overall survival (OS, HR = 1.22, 95% CI = 1.03-1.45) (**Figure 1C**); ICOSL expression in TNBC was related to relapse-free survival (RFS, HR = 1.47, 95% CI = 1.01-2.12) (**Figure 1D**) but not overall survival (data not shown).

*Regulatory T cells (Tregs) were positively correlated with ICOSL expression, as demonstrated by TNBC database analyses*

The abundance of only 3 out of 22 immune cell types was significantly altered in the ICOSL expression groups (**Figure 2A**), including Tregs, and the abundance of 10 out of 22 immune cell types was positively correlated with ICOSL expression, including Tregs (**Figure 2B**). Activated mast cells, resting myeloid dendritic cells, and resting CD4+ T memory cells showed the highest negative Spearman correlation with ICOSL expression (**Figure 2C-E**). Moreover, Tregs and follicular helper T cells (**Figure 2F, 2G**)

## ICOSL enhances tumor progression in TNBC

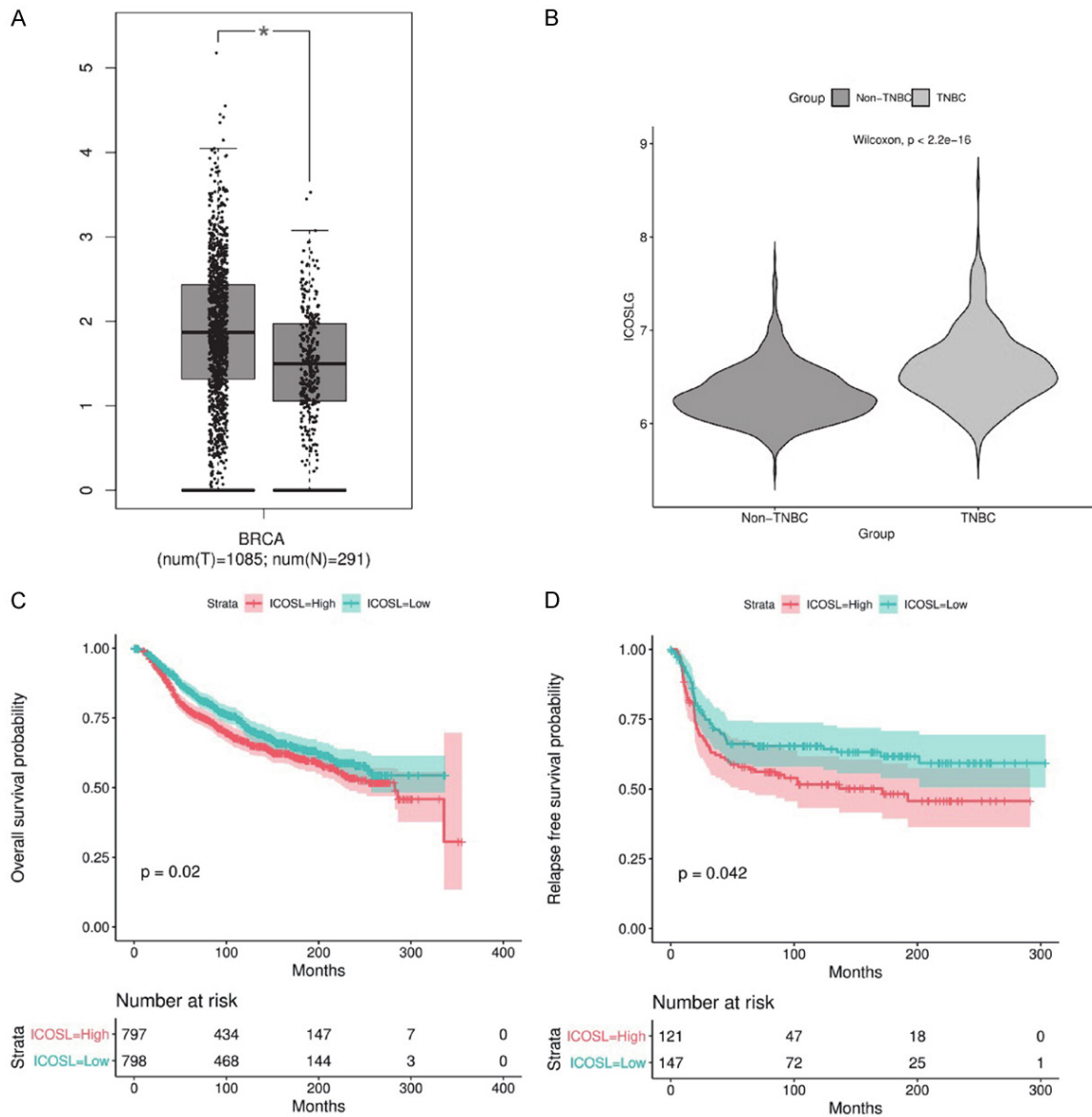


**Figure 1.** ICOSL expression and survival curves in breast cancer and TNBC datasets. A. ICOSL mRNA expression in patients with breast cancer and healthy individuals. B. ICOSL mRNA expression in patients with TNBC and patients with non-TNBC. C. Overall survival curve for the high and low ICOSL expression groups among all breast cancer types in TCGA. D. Relapse-free survival curve for the high and low ICOSL expression groups in TNBC in TCGA.

were positively correlated with ICOSL expression.

*ICOSL expressed on the TNBC cell line enhanced tumor cell growth through induction of Foxp3+ Treg differentiation in vitro*

Overexpression lentiviruses were successfully constructed, and ICOSL protein expression in MDA-MB-231 cells infected with ICOSL-OE lentiviruses was significantly higher than that in the control group (PCR, western blotting and

flow cytometry in **Figure 3A-C**). MDA-MB-231 cells infected with ICOSL-control lentivirus were sorted for ICOSL negativity and used as MDA-MB-231-control cells in all the following experiments (**Figure 3C**). The flow chart is shown in **Figure 3D**. PBMCs were collected from a volunteer, the MHC type was determined by HLA-A0201 antibody, and the CD4+ T cells were sorted. Furthermore, MDA-MB-231 cells were cocultured with CD4+ T cells obtained from the volunteer mentioned above. After 7 days of cul-

# ICOSL enhances tumor progression in TNBC

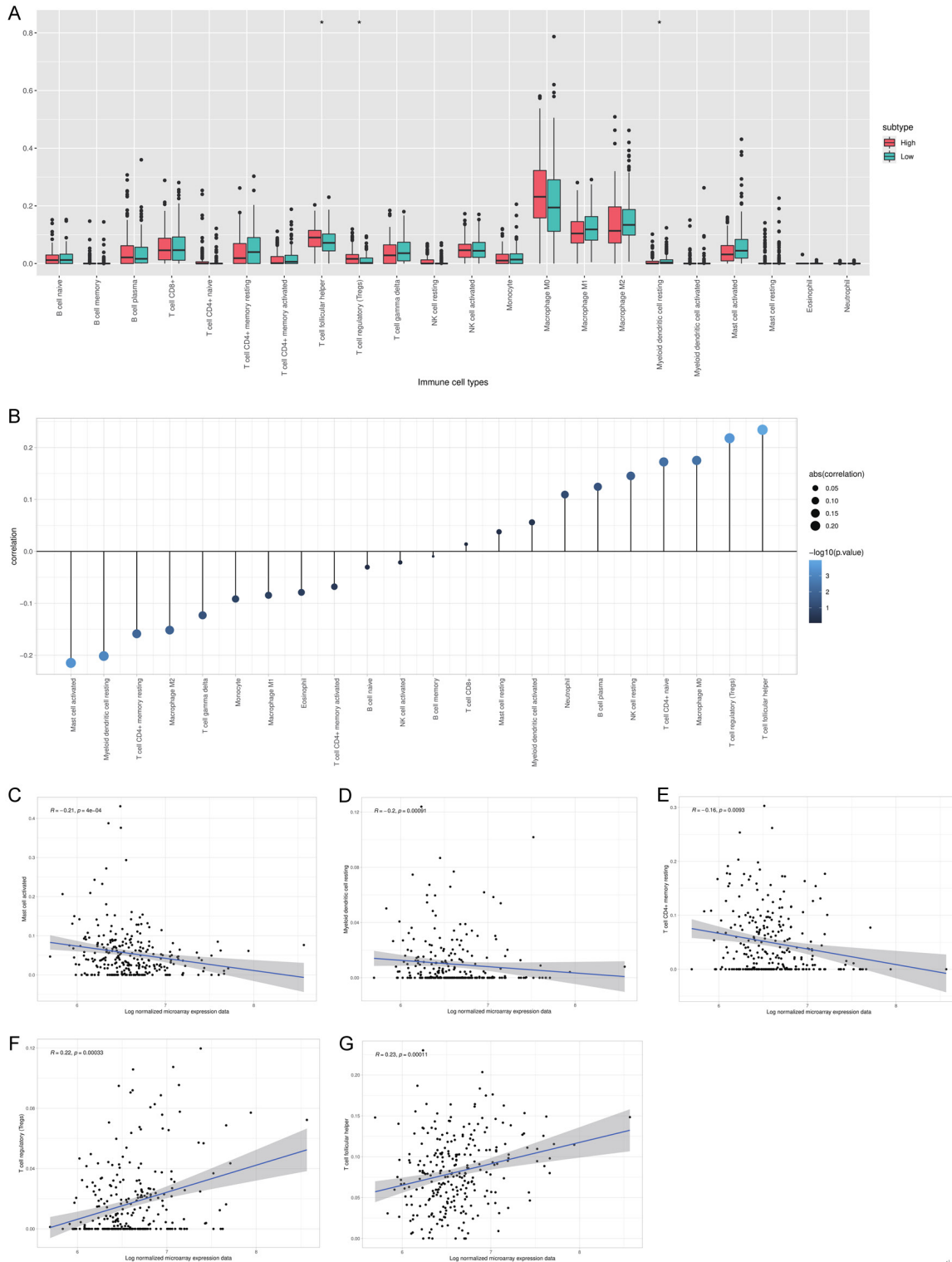


**Figure 2.** Immune infiltration analysis of the TNBC dataset. A. Estimated immune cell abundance distribution for the high and low ICOSL expression groups (\* $p < 0.01$ ). B. Lollipop plot of the Spearman correlation between ICOSL expression and estimated immune cell abundance. C-E. Scatter plot of the top three negative correlations between ICOSL expression and estimated immune cell abundance. F, G. Scatter plot of the top three positive correlations between ICOSL expression and estimated immune cell abundance.

# ICOSL enhances tumor progression in TNBC

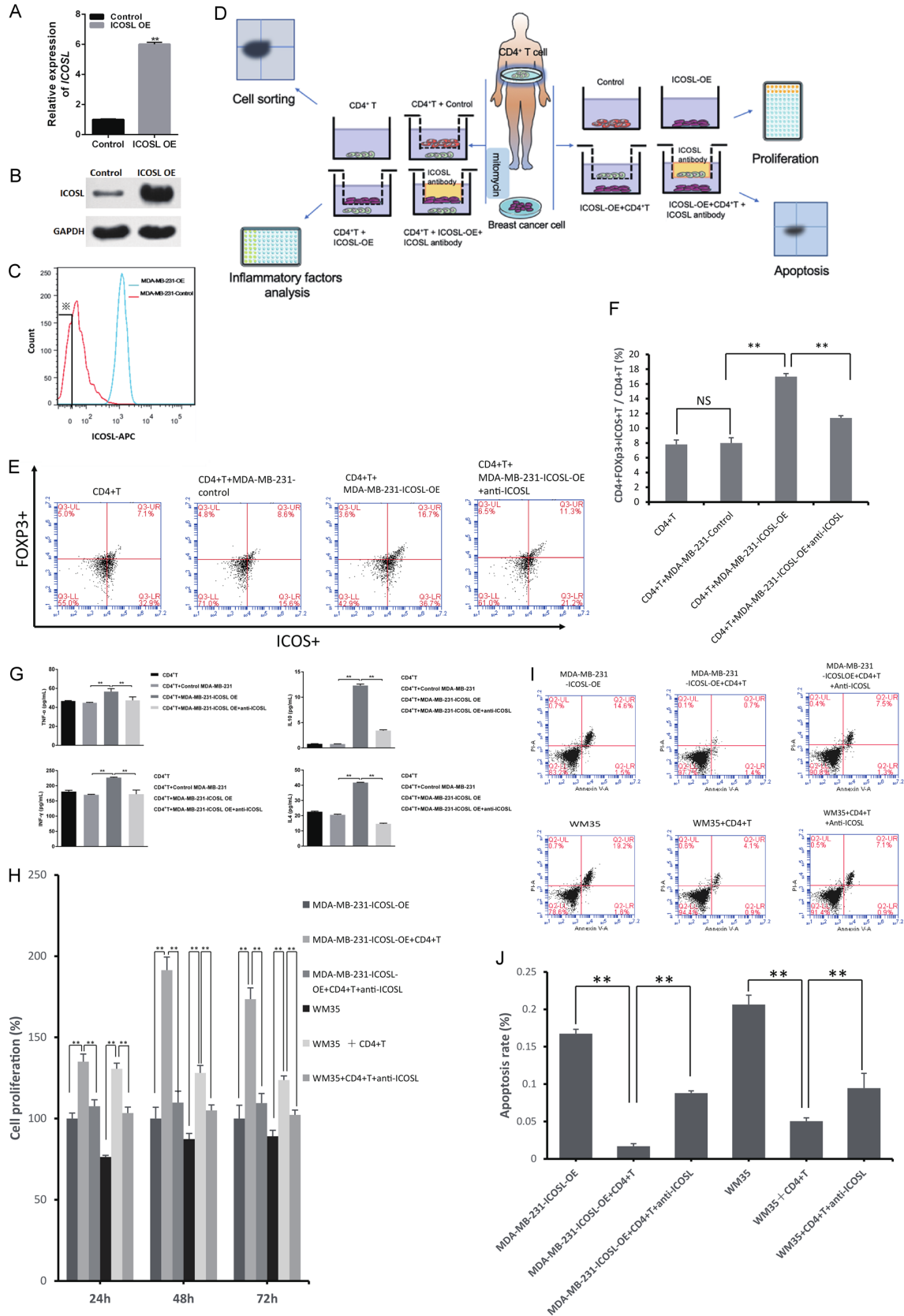


**Figure 3.** ICOSL expressed on TNBC cells can induce the differentiation of Foxp3+ Treg cells, enhancing tumor cell growth and suppressing apoptosis in vitro. MDA-MB-231 cells were infected with ICOSL overexpression lentivirus

## ICOSL enhances tumor progression in TNBC

and negative control lentivirus. The specificity and efficiency were validated by (A) quantitative reverse transcription polymerase chain reaction (qRT-PCR), (B) western blotting and (C) flow cytometry analysis. ※, MDA-MB-231 cells were sorted for ICOSL-negative MDA-MB-231 cells to be used as MDA-MB-231-control cells, which were used in all the following experiments. (D) Flow charts of our in vitro experiment. (E, F) After 7 days of cultivation with MDA-MB-231 cells, the rate of FOXP3<sup>+</sup>/ICOS<sup>+</sup> T cells among CD4<sup>+</sup> T cells was analyzed via flow cytometry. \*\*P<0.05. (G) The levels of TNF- $\alpha$ , IFN- $\gamma$ , IL-10, and IL-4 in cell culture supernatants measured with an ELISA kit (\*\*P<0.05). Each experiment was repeated three times. (H-J) MDA-MB-231 ICOSL-OE cells and WM35 melanoma cells ( $3 \times 10^6$ /mL) were cocultured with CD4<sup>+</sup> T cells ( $1 \times 10^6$ /mL). After 7 days, cell proliferation (H) and apoptosis assays (I, J) of tumor cells were conducted. Each experiment was repeated three times (\*\*, P<0.05).

tivation, the rate of FOXP3<sup>+</sup>/ICOS<sup>+</sup> T cells among CD4<sup>+</sup> T cells was analyzed by flow cytometry. We found that the proportion of FOXP3<sup>+</sup>/ICOS<sup>+</sup> T cells among CD4<sup>+</sup> T cells increased significantly after coculture of MDA-MB-231-ICOSL-OE cells with CD4<sup>+</sup> T cells compared with coculture of MDA-MB-231-control cells with CD4<sup>+</sup> T cells. The proportion of FOXP3<sup>+</sup>/ICOS<sup>+</sup> T cells decreased significantly after treatment with ICOSL antibody (**Figure 3E, 3F**, P<0.05). These results show that TNBC cells expressing ICOSL can promote the activation and expansion of Treg cells and that blocking the ICOS-ICOSL pathway can inhibit this process.

The levels of the cytokines TNF- $\alpha$ , IFN- $\gamma$ , IL-10, and IL-4 in the supernatant were also measured. We found that the levels of the TNF- $\alpha$ , IFN- $\gamma$ , IL-10, and IL-4 cytokines were significantly elevated when CD4<sup>+</sup> T cells were cocultured with MDA-MB-231-OE cells compared with CD4<sup>+</sup> T cells cocultured with MDA-MB-231-control cells, especially IL-10 (from  $0.81 \pm 0.04$  pg/mL to  $12.31 \pm 0.29$  pg/mL) and IL-4 (from  $22.61 \pm 0.4$  pg/mL to  $41.76 \pm 0.22$  pg/mL) (**Figure 3G**, P<0.05). Additionally, blocking ICOSL with a monoclonal antibody significantly inhibited the secretion of those cytokines, especially IL-10 (from  $12.31 \pm 0.29$  pg/mL to  $3.42 \pm 0.14$  pg/mL) and IL-4 (from  $41.76 \pm 0.22$  pg/mL to  $14.44 \pm 0.40$  pg/mL) (**Figure 3G**, P<0.05). It is worth noting that both IL-10 and IL-4 are Th2-type cytokines. Th2 immune responses form a favorable environment for tumor cell growth, and IL-10 is a potent inhibitor of antitumor immune responses. The results indicate that ICOSL overexpression in MDA-MB-231 cells promoted T cells to secrete Th2-type cytokines, including IL-10 and IL-4.

To confirm the contribution of the CD4<sup>+</sup> T cells to the proliferation and apoptosis of ICOSL-positive MDA-MB-231 cells, CD4<sup>+</sup> T cells were collected from HLA-A0201 volunteers and

cocultured with MDA-MB-231-ICOSL-OE cells. Cell proliferation and apoptosis assays were conducted. Martin-Orozco N [29] showed that WM35 melanoma cells express high levels of ICOS-L. ICOS-L expression by melanoma tumor cells can directly drive Treg activation and expansion in the tumor microenvironment as another mechanism of immune evasion. Here, WM35 cells were used in our study as a control. The groups were as follows: 1. MDA-MB-231 ICOSL-OE cells; 2. MDA-MB-231 ICOSL-OE cells + CD4<sup>+</sup> T cells; 3. MDA-MB-231 ICOSL-OE cells + CD4<sup>+</sup> T cells + anti-ICOSL antibody; 4. WM35 cells; 5. WM35 cells + CD4<sup>+</sup> T cells; 6. WM35 cells + CD4<sup>+</sup> T cells + anti-ICOSL antibody (**Figure 3H-J**). We found that ICOSL promoted tumor cell proliferation when CD4<sup>+</sup> T cells were cocultured with MDA-MB-231-ICOSL-OE or WM35 cells compared with MDA-MB-231-ICOSL-OE or WM35 cells only. This effect was inhibited by the ICOSL antibody (**Figure 3H**, P<0.05). ICOSL inhibited tumor cell MDA-MB-231-ICOSL-OE/WM35 cell apoptosis when CD4<sup>+</sup> T cells were cocultured with tumor cells compared with tumor cells only. Apoptosis was enhanced when the ICOSL antibody was used (**Figure 3I, 3J**, P<0.05). The results show that ICOSL expression by both MDA-MB-231-ICOSL-OE TNBC cells and WM35 melanoma tumor cells can enhance proliferation and suppress apoptosis when cocultured with CD4<sup>+</sup> T cells.

*ICOSL expressed on the TNBC cell line was correlated with the extracellular matrix (ECM) and p38 pathway*

We identified 600 DEGs associated with ICOSL expression (**Supplementary Figure 1A, 1B**). Functional annotation indicated that the DEGs were closely related to the ECM and cell cycle (**Supplementary Figure 1C, 1D**). We confirmed the functional annotation pathway using Reactome GSEA (**Supplementary Figure 1E-J**). The PPI network of the DEGs is shown in **Supplementary Figure 2A**. Moreover, we used

## ICOSL enhances tumor progression in TNBC

the MCODE algorithm to obtain a significant module from the PPI network ([Supplementary Figure 2B](#)). Thirty-three genes in the significant module were identified as hub genes. We noticed that the module comprised two sub-clusters, which were characterized by up- or downregulated genes. Therefore, we further divided the significant modules into two clusters and performed KEGG enrichment analysis. One cluster (15 downregulated and 2 upregulated genes) was associated with ECM-receptor interactions and focal adhesions. The other cluster (16 upregulated genes) was associated with the cell cycle, DNA replication, and ubiquitin-mediated proteolysis ([Supplementary Figure 2C](#)).

Many studies have shown that the p38 MAPK signaling pathway in many tumors, such as breast cancer, may contribute to excessive ECM production, which is correlated with the growth and progression of tumor cells [29-31]. Our previous research also showed that P-p38 MAPK expression was significantly associated with clinicopathological factors and that PR/HER2 might be associated with the phosphorylation of p38 MAPK in different types of breast cancer [32].

To further determine the correlation between ICOSL and the p38 pathway, we analyzed the expression of the 4 subtypes of p38-MAPK genes, MAPK11, MAPK12, MAPK13, and MAPK14, and 33 upstream and downstream genes in the p38 pathway. We found that only MAPK12, MAP2K3, and MAPKAPK2 were significantly upregulated in the high ICOSL expression group and were significantly correlated with ICOSL expression ([Figure 4A-H](#),  $P < 0.05$ ), indicating that p38 pathway activation might be associated with ICOSL expression. The data of other genes that were not significantly correlated with ICOSL expression are not shown here. We also downloaded TNBC data from TCGA and found that, among the 4 subtypes of p38-MAPK, MAPK13 and MAPK14 were significantly upregulated in the high ICOSL expression group, with correlation coefficients  $R$  of 0.26 and 0.36, respectively, while MAPK11 and MAPK12 were not significantly upregulated ([Figure 4I-P](#),  $P < 0.05$ ). Furthermore, we examined the phosphorylation status of p38 proteins (MAPK11, MAPK12, MAPK13, and MAPK14) with respect to breast cancer in the

qPTM database and found that MAPK13 (position 182) and MAPK14 (position 182) have significantly higher phosphorylation status in breast cancer [33, 34]. However, MAPK13 (position 350) has a lower phosphorylation status in breast cancer [34, 35].

All of these results indicate that ICOSL expression might be associated with p38-MAPK pathway activation. However, which p38 subtype might be activated needs further study.

### *ICOSL promotes p38 phosphorylation in vitro*

Next, we analyzed the effect of ICOSL overexpression on protein kinase phosphorylation in tumor cells using a proteome profiler human phospho kinase array kit. This is a membrane-based antibody array for parallel determination of the relative levels of human protein kinase phosphorylation that can simultaneously detect the phosphorylation of 43 human kinases and the total amounts of 2 related proteins.

MDA-MB-231 ICOSL-OE cells were cocultured with CD4+ T cells for 7 days to induce FOXP3+ Treg cells. CD4+ T cells were collected and cocultured with MDA-MB-231-control and MDA-MB-231 ICOSL-OE cells. After incubation at 37°C for 48 h, MDA-MB-231-control and MDA-MB-231-ICOSL-OE cells were collected, and the levels of human protein kinase phosphorylation in tumor cells were analyzed using the phosphorylated tissue microarray ([Figure 5A, 5B](#)). The results showed that 12 protein kinase phosphorylation levels, especially factors in the p38-MAPK pathway, such as p38 (T180/Y182), p53 (S392), p53 (S46), and CREB (S133) were obviously upregulated.

Then, to further determine whether ICOSL promotes p38 phosphorylation in vitro, we engaged MDA-MB-231 rhICOS-Fc cells to activate ICOSL instead of CD4+ T cells. MDA-MB-231-Con and MDA-MB-231-ICOSL-OE cells were inoculated into 6-well plates, and rhICOS-Fc was added. After incubation for 48 h, the protein expression levels of p38 and p-p38 were detected via western blotting. The results showed that the intracellular p38 phosphorylation level in MDA-MB-231 ICOSL-OE cells was increased significantly when rhICOS-Fc was used. The intracellular p38 phosphorylation level decreased when SB202190 was added ([Figure 5C](#),  $P < 0.05$ ).

## ICOSL enhances tumor progression in TNBC

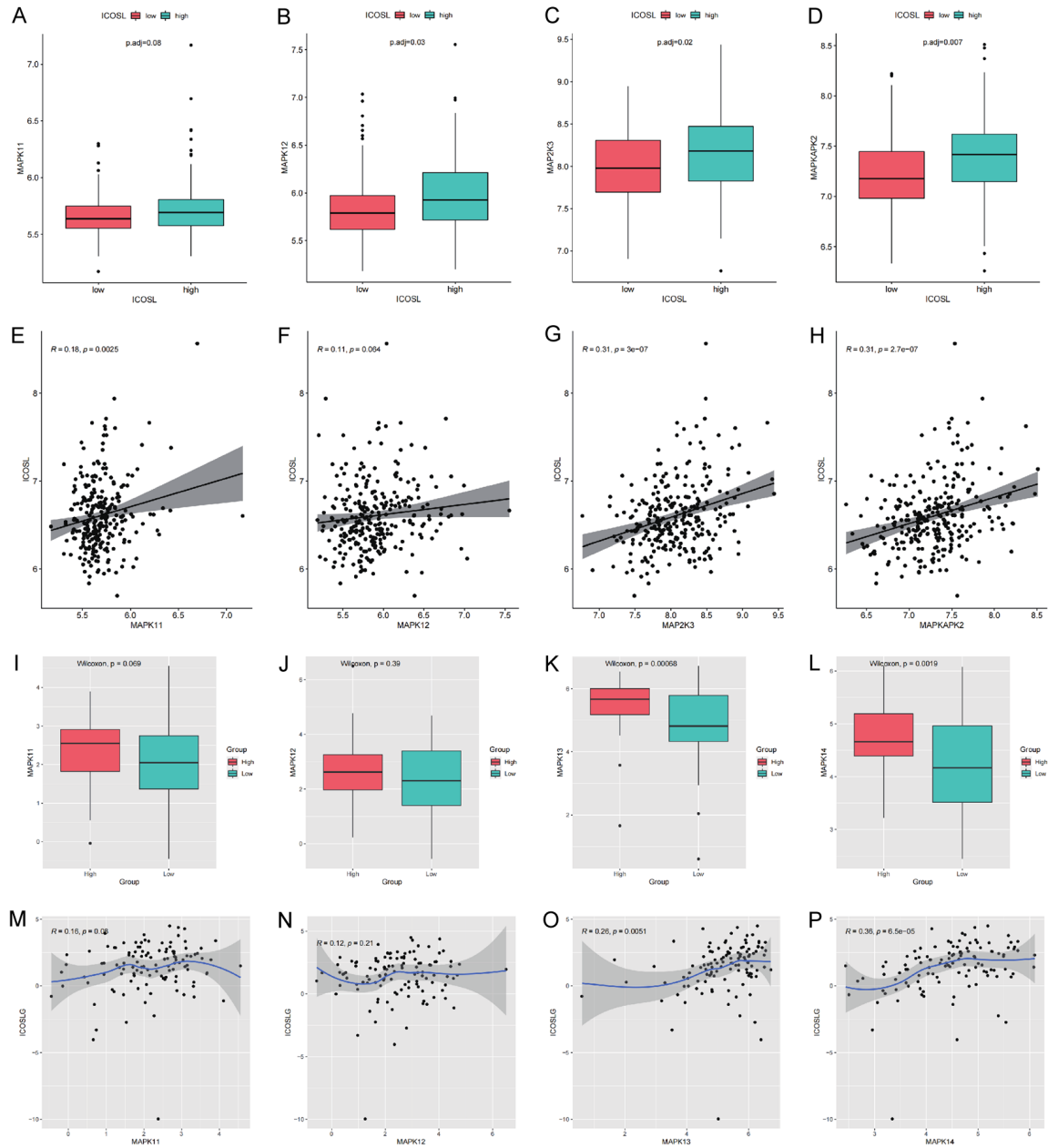


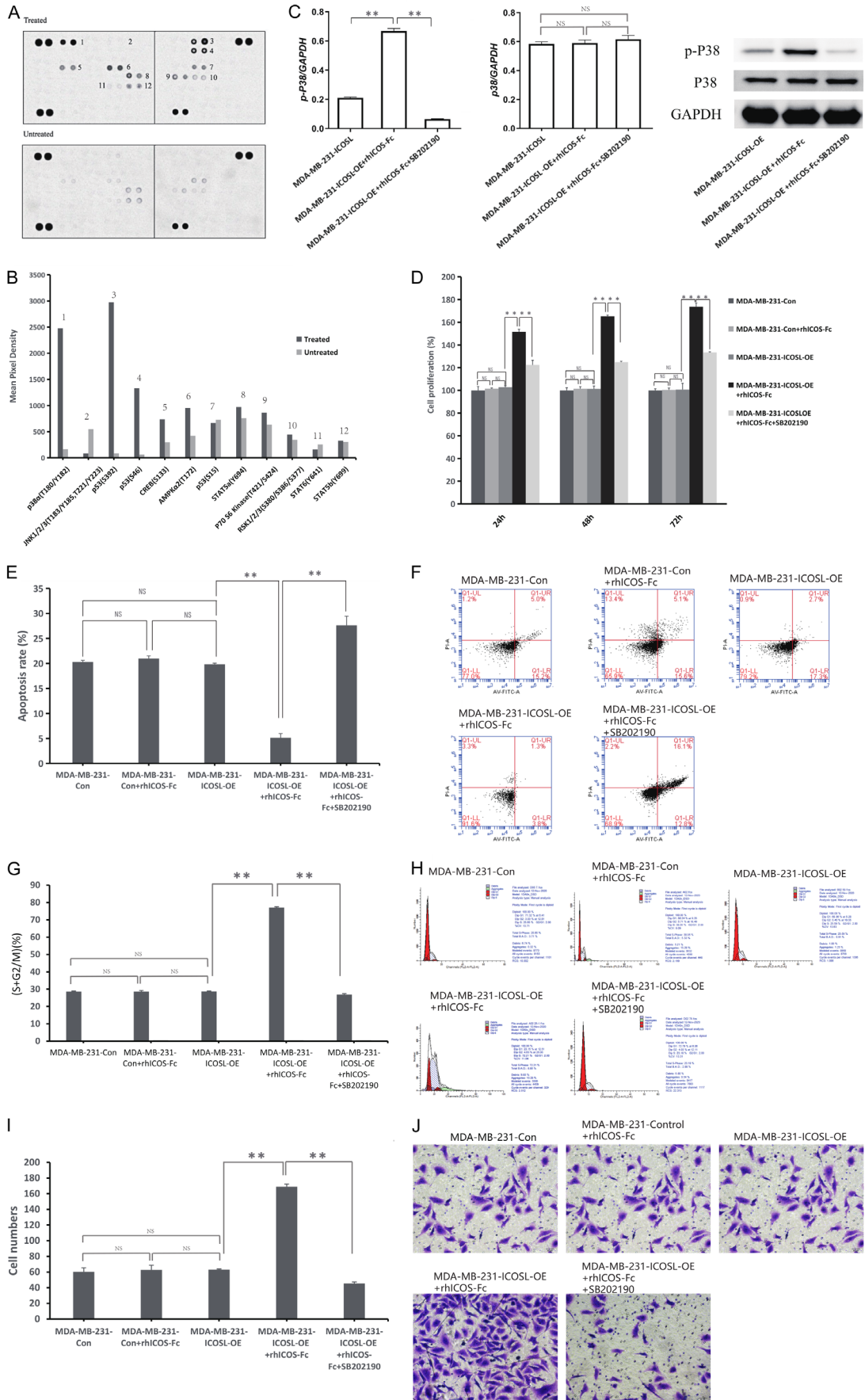
**Figure 4.** Analysis of DEGs related to p38 MAP kinase. A-D. Boxplots of p38 MAP kinase, MAP2K3 and MAPKAPK2 expression in the high and low ICOSL expression groups were generated, with the median value determined according to the method mentioned in 2.1.4 serving as the cutoff value. E-H. Scatter plot of p38 MAP kinase, MAP2K3, and MAPKAPK2 expression and ICOSL expression ( $*P < 0.05$ ). I-L. Boxplots of p38 MAP kinase expression in the high and low ICOSL expression groups were generated using the median value according to TCGA data as the cutoff value. M-P. Scatter plot of p38 MAP kinase and ICOSL expression.

*ICOSL promotes tumor progression by phosphorylating p38 in vitro*

Next, we engaged MDA-MB-231 rhICOS-Fc cells to activate ICOSL to further determine the role of ICOSL in tumor proliferation, apoptosis migration, and the proliferation cycle and whe-

ther p38 phosphorylation is related to these processes. As a result, the proliferation (Figure 5D), proportion of tumor cells in the proliferation cycle (Figure 5G, 5H) and migration (Figure 5I, 5J) were significantly promoted ( $P < 0.05$ ). In contrast, tumor cell apoptosis (Figure 5E, 5F) decreased significantly when the ICOS receptor

# ICOSL enhances tumor progression in TNBC



## ICOSL enhances tumor progression in TNBC

**Figure 5.** ICOSL promoted tumor progression by phosphorylating p38 in vitro. (A, B) Phosphokinase array experiments. The results showed that CD4<sup>+</sup> T cells cocultured with MDA-MB-231 ICOSL-OE cells could change 12 protein kinase phosphorylation levels, especially p38 (T180/Y182), p53 (S392), p53 (S46), and CREB (S133), which are all in the p38-MAPK pathway. (C) The protein expression levels of p38 and p-p38 were detected by western blotting. The intracellular p38 phosphorylation level in MDA-MB-231 ICOSL-OE cells was increased significantly when rhICOS-Fc was used. The intracellular p38 phosphorylation level decreased when SB202190 was added (\*\*, P<0.05). (D-J) The proliferation (D), proportion of tumor cells in the proliferation cycle (G, H) and migration (I, J) were significantly promoted (\*\*, P<0.05). In contrast, tumor cell apoptosis (E, F) decreased significantly when ICOS was provided via ICOS fusion protein (\*\*, P<0.05). The above processes were significantly inhibited by the addition of the p38 inhibitor SB202190 (D-J, \*\*, P<0.05). All of the above experiments were repeated three times.

was provided by rhICOS-Fc. The above processes were significantly inhibited by addition of the p38 inhibitor SB202190 (P<0.05).

*In vivo experiments in a nude mouse model showed that TNBC growth was enhanced by ICOSL and activated by ICOS*

H9 cells were used to provide ICOS receptors in the following MDA-MB-231 breast cancer mouse model. The ICOS-OE lentivirus and negative control lentivirus were constructed and used to infect H9 cells for 72 h. Both western blotting and flow cytometry showed that ICOS protein expression increased significantly (**Figure 6A-C**). ICOS-negative ICOS-control lentivirus cells were sorted and used as H9-control cells in the mouse model (**Figure 6C**).

In addition, to study the role of ICOSL on tumor cells in vitro before in vivo experiments, ICOS-overexpressing H9 cells were used to provide ICOS receptors to activate ICOSL. H9 cells infected with control lentivirus or ICOSL-OE lentivirus were treated with 40 µg/mL mitomycin for 2 h and were cocultured with MDA-MB-231 cells for 72 h. Tumor cell proliferation, apoptosis, migration, and invasion experiments were conducted in vitro. When ICOS was provided by H9-ICOS cells, the proliferation, migration, and proportion of tumor cells in the proliferation cycle were significantly increased and tumor cell apoptosis significantly decreased (data not shown).

Then, in vivo experiments were conducted. A nude mouse model of TNBC was established with MDA-MB-231 cells as the tumor cells, as mentioned in 2.2.12. The mice were divided into 4 groups as follows: 1. MDA-MB-231-Con + H9-Con; 2. MDA-MB-231-Con + H9-ICOS-OE; 3. MDA-MB-231-ICOSL-OE + H9-Con; and 4. MDA-MB-231-ICOSL-OE + H9-ICOS-OE.

From Day 7 after the injection of MDA-MB-231 cells, the mice were closely monitored every 3 days, and the tumor volume was measured. The tumor volume of group 4 is significantly higher than the other 3 group and tumor volume of group 3 is significantly higher than the group 1 and 2 thereafter day 22 (**Figure 6D**, \*P<0.05).

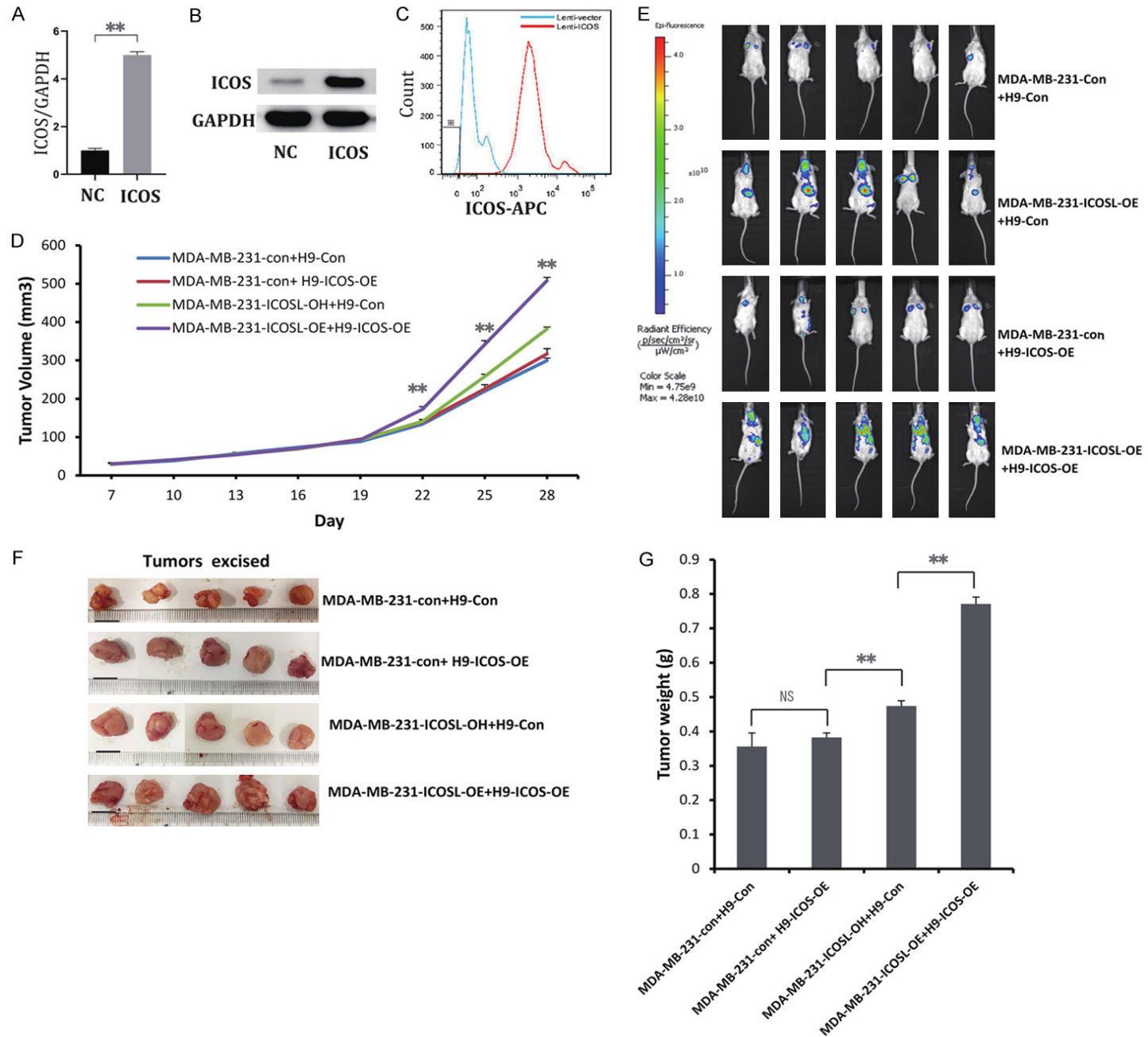
Five weeks after tumor cell inoculation, in vivo imaging analysis was performed, and the tumor load in Group 4 (H9-ICOS-OE cells engaged with MDA-MB-231-ICOSL-OE cells) was the largest among all four groups (**Figure 6E**). The mice were sacrificed on Day 35, and the tumors were excised. Both tumor volume and weight were the largest in Group 4 among all 4 groups (**Figure 6F, 6G**). These results indicate that tumor progression was promoted by the expression of ICOSL in a TNBC nude mouse model.

### Discussion

To date, there has been little research on ICOSL expression in TNBC, its mechanism, and its effect on proliferation. Costimulatory molecules are expressed on T cells. Costimulatory molecular ligands are expressed in APC cells. At present, most studies mainly focus on the effects of costimulatory molecules on T cells, but there are few studies on the effects of costimulatory molecular ligands on the intracellular signaling pathways in APC cells. The effect of ICOSL expression on the intracellular signaling pathway in TNBC cells has not been reported. Our results are the first to show that ICOSL overexpression in TNBC cells can stimulate the ICOS<sup>+</sup> Treg cell differentiation of CD4<sup>+</sup> T cells. We also found that ICOSL overexpression in TNBC cells could reverse the p38 pathway to promote tumor progression.

ICOSL was discovered mostly in APCs and cancer cells, such as gastric carcinoma, melano-

# ICOSL enhances tumor progression in TNBC



## ICOSL enhances tumor progression in TNBC

**Figure 6.** In vivo experiments in nude mouse models showed that TNBC growth was enhanced by ICOSL activated by the ICOS receptor. (A-C) H9 cells were inoculated into 6-well plates at  $1 \times 10^5$ /well and infected with ICOS overexpression lentivirus or negative control lentivirus for 72 h. The specificity and efficiency were validated by western blotting and quantitative reverse transcription polymerase chain reaction (qRT-PCR). (\*\*,  $P < 0.05$ ). ※, H9-ICOS-negative cells were sorted and used as H9-control cells in the experiment. (D-G) In vivo experiments in a nude mouse model. (D) The tumor volume of group 4 of MDA-MB-231-ICOSL-OE + H9-ICOS-OE is significantly higher than the other 3 groups and tumor volume of group 3 of MDA-MB-231-ICOSL-OE + H9-Con is significantly higher than the group 1 and 2 thereafter day 22 (\*,  $P < 0.05$ ). (E) Five weeks after tumor cell inoculation, in vivo imaging analysis was performed, and the tumor load in Group 4 (H9-ICOS-OE cells treated with MDA-MB-231-ICOSL-OE cells) was the largest among all four groups. (F, G) The mice were sacrificed on Day 35, and the tumors were excised (\*\*,  $P < 0.05$ ).

ma, and hematologic neoplasm cells [14, 15, 36]. In a sense, tumor cells can be used as APCs to directly drive Treg activation as a method of immune evasion. The expression of ICOSL on TNBC MDA-MB-231 cells was detected first, and MDA-MB-231 cells had very low expression of ICOSL (**Figure 3C**). Therefore, we induced ICOSL overexpression in TNBC MDA-MB-231 cells and conducted ICOSL-negative sorting of cells transfected with control plasmid to mimic ICOSL-positive and ICOSL-negative TNBC cells, respectively, instead of using different ICOSL-positive TNBC cell lines. The melanoma cell line WM35 was also used in our study as a control to confirm the contribution of CD4<sup>+</sup> T cells to the proliferation and apoptosis of ICOSL-positive MDA-MB-231 cells.

In our previous investigation, we found that ICOSL overexpression is associated with poor prognosis and may be a novel prognostic factor in breast cancer [37]. Published studies have also shown that ICOS is associated with poor prognosis in breast cancer because it promotes the amplification of CD4<sup>+</sup> T cells [38]. Our study further explored the effect of ICOSL overexpression on TNBC cell proliferation. Our results suggested that the proliferation ability of MDA-MB-231 ICOSL-OE cells increased even more than that of MDA-MB-231 ICOSL-negative cells after the addition of CD4<sup>+</sup> T cells.

This study also revealed that ICOSL overexpression in breast cancer cells stimulated the ICOS<sup>+</sup> Treg cell differentiation of CD4<sup>+</sup> T cells obtained from PBMCs of HLA-A2-type volunteers. Our group previously found that blocking the ICOS/ICOSL pathway in mouse hematological tumor cells led to downregulation of the anti-inflammatory factors IL-4 and IL-10 [37]. IL-10 is a potent inhibitor of antitumor immune responses, and Th2 immune responses form a favorable environment for the growth of tumors. In our study, we found that ICOSL pro-

moted T cells to secrete inflammatory factors, especially the anti-inflammatory factors IL-10 and IL-4. It was supposed that both Th1 and Th2 responses in breast cancer are activated by ICOS/ICOSL signaling to regulate immune cell responses against tumors, especially Th2 responses.

In addition, our study showed that the application of an ICOSL antibody inhibited Treg cell differentiation, the secretion of tumor-promoting factors, and tumor cell proliferation. Similar to our research, a previous study on tumor vaccines found that ICOS blockade induces better antitumor activity than vaccination alone in a mouse prostate cancer model [39]. The tumor size in the group treated with ICOS blockade was much smaller than that in the vaccine with IgG mAb group. In addition, more immune-suppressing Tregs infiltrated the tumor after treatment with the tumor vaccine. It is known that the ICOS-ICOSL pathway is blocked not only on Treg cells that are associated with Th2-type cytokines but also on CD8<sup>+</sup> CTLs that have an antitumor effect associated with Th1-type cytokines. Therefore, ICOSL may play distinct roles in different cell types. Our results confirmed the immunosuppressive effect caused by ICOSL overexpression in patients with TNBC, which provides a theoretical basis for the treatment of ICOSL-overexpressing TNBC.

To further identify the pathway that affects ICOSL expression, we found that p38 pathway activation is highly correlated with ICOSL expression by analyzing a database dataset. However, the specific correlation between ICOSL and p38 phosphorylation is not yet fully understood. Han et al. noted that ICOSL expression in acute myeloid leukemia (AML) cells promotes Treg expansion and that IL-10 promotes AML cell proliferation through the p38 pathway [40]. P38 MAPK includes four subtypes, p38  $\alpha$  (MAPK14), p38  $\beta$  (MAPK11), p38

## ICOSL enhances tumor progression in TNBC

$\gamma$  (MAPK12), and p38  $\delta$  (MAPK13). Our phosphokinase array and in vitro experimental results showed that ICOSL activation in TNBC promoted tumor proliferation and invasion through p38 phosphorylation. After application of the p38 inhibitor SB202190, these biological behaviors were reversed. Our study showed that ICOSL overexpression promoted p38  $\alpha$  phosphorylation levels. However, the specific signaling pathways activated by ICOSL need to be further studied.

In this study, we used only one breast cancer cell line that weakly expressed ICOSL. To explain the role of ICOSL as much as possible, ICOSL-overexpressing MDA-MB-231 cells were constructed, and we sorted ICOSL-negative MDA-MB-231 cells for use as control cells. Moreover, to explain the effect of ICOSL on Tregs to the greatest extent, we used melanoma cells as a control. However, the specific signaling pathways activated by ICOSL need to be further studied.

Overall, our study demonstrated that ICOSL expressed in TNBC enhances tumor cell growth by inducing Foxp3+ Treg cell differentiation and reversing p38 activation. Our results provide a theoretical basis for future TNBC therapy targeting ICOSL.

### Acknowledgements

This work was supported in part by a grant from the National Natural Science Foundation of China (NSFC No. 81472479) to Bin Wang, National Natural Science Foundation of China (NSFC No. 82002122) and Changning district medical and health research projects of Shanghai (CNKW2018Y35) to Ning Ma, and the Natural Science Foundation of Shanghai to Yingyi Zhang (19ZR1456200).

The Ethics Committee of Changhai Hospital granted approval (#20140310) for this research protocol. It was confirmed that all necessary consent, including the consent to participate in the study and the consent to publish, were obtained from every patient involved in this study.

### Disclosure of conflict of interest

None.

**Address correspondence to:** Bin Wang and Yajie Wang, Department of Oncology, Changhai Hospital, Naval Medical University, 168 Changhai Road, Shanghai 200433, P. R. China. Tel: +86-137-64528043; E-mail: qcwangb@163.com (BW); Tel: +86-13901846936; E-mail: yajiewa0459@163.com (YJW); Dongxun Zhou, Department of Endoscopy and Gastroenterology, Eastern Hepatobiliary Hospital, Naval Medical University, 225 Changhai Road, Shanghai 200433, P. R. China. Tel: +86-13482449963; E-mail: dongxunzhou@163.com

### References

- [1] Zhang R, Yang Y, Dong W, Lin M, He J, Zhang X, Tian T, Yang Y, Chen K, Lei QY, Zhang S, Xu Y and Lv L. D-mannose facilitates immunotherapy and radiotherapy of triple-negative breast cancer via degradation of PD-L1. *Proc Natl Acad Sci U S A* 2022; 119: e2114851119.
- [2] Harbeck N, Penault-Llorca F, Cortes J, Gnani M, Houssami N, Poortmans P, Ruddy K, Tsang J and Cardoso F. Breast cancer. *Nat Rev Dis Primers* 2019; 5: 66.
- [3] Garrido-Castro AC, Lin NU and Polyak K. Insights into molecular classifications of triple-negative breast cancer: improving patient selection for treatment. *Cancer Discov* 2019; 9: 176-198.
- [4] Xie D, Li S, Wu T, Wang X and Fang L. MiR-181c suppresses triple-negative breast cancer tumorigenesis by targeting MAP4K4. *Pathol Res Pract* 2022; 230: 153763.
- [5] Wang C, Kar S, Lai X, Cai W, Arfuso F, Sethi G, Lobie PE, Goh BC, Lim LHK, Hartman M, Chan CW, Lee SC, Tan SH and Kumar AP. Triple negative breast cancer in Asia: an insider's view. *Cancer Treat Rev* 2018; 62: 29-38.
- [6] Boire A, Brastianos PK, Garzia L and Valiente M. Brain metastasis. *Nat Rev Cancer* 2020; 20: 4-11.
- [7] Loi S, Drubay D, Adams S, Pruneri G, Francis PA, Lacroix-Triki M, Joensuu H, Dieci MV, Badve S, Demaria S, Gray R, Munzone E, Lemonnier J, Sotiriou C, Piccart MJ, Kellokumpu-Lehtinen PL, Vingiani A, Gray K, Andre F, Denkert C, Salgado R and Michiels S. Tumor-infiltrating lymphocytes and prognosis: a pooled individual patient analysis of early-stage triple-negative breast. *J Clin Oncol* 2019; 37: 559-569.
- [8] Qin G, Wang X, Ye S, Li Y, Chen M, Wang S, Qin T, Zhang C, Li Y, Long Q, Hu H, Shi D, Li J, Zhang K, Zhai Q, Tang Y, Kang T, Lan P, Xie F, Lu J and Deng W. NPM1 upregulates the transcription of PD-L1 and suppresses T cell activity in triple-negative breast cancer. *Nat Commun* 2020; 11: 1669.

## ICOSL enhances tumor progression in TNBC

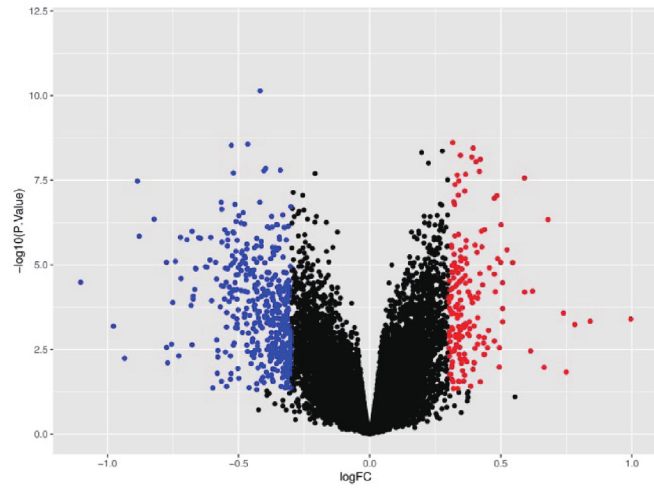
- [9] Jia H, Truica CI, Wang B, Wang Y, Ren X, Harvey HA, Song J and Yang JM. Immunotherapy for triple-negative breast cancer: existing challenges and exciting prospects. *Drug Resist Updat* 2017; 32: 1-15.
- [10] Li W, Tanikawa T, Kryczek I, Xia H, Li G, Wu K, Wei S, Zhao L, Vatan L, Wen B, Shu P, Sun D, Kleer C, Wicha M, Sabel M, Tao K, Wang G and Zou W. Aerobic glycolysis controls myeloid-derived suppressor cells and tumor immunity via a specific CEBPB isoform in triple-negative breast cancer. *Cell Metab* 2018; 28: 87-103.
- [11] Geltink RIK, Kyle RL and Pearce EL. Unraveling the complex interplay between T cell metabolism and function. *Annu Rev Immunol* 2018; 36: 461-488.
- [12] Bour-Jordan H, Esensten JH, Martinez-Llordella M, Penaranda C, Stumpf M and Bluestone JA. Intrinsic and extrinsic control of peripheral T-cell tolerance by costimulatory molecules of the CD28/B7 family. *Immunol Rev* 2011; 241: 180-205.
- [13] Panneton V, Chang J, Witalis M, Li J and Suh WK. Inducible T-cell co-stimulator: signaling mechanisms in T follicular helper cells and beyond. *Immunol Rev* 2019; 291: 91-103.
- [14] Liu D, Xu H, Shih C, Wan Z, Ma X, Ma W, Luo D and Qi H. T-B-cell entanglement and ICOSL-driven feed-forward regulation of germinal centre reaction. *Nature* 2015; 517: 214-218.
- [15] Amatore F, Gorvel L and Olive D. Role of Inducible Co-Stimulator (ICOS) in cancer immunotherapy. *Expert Opin Biol Ther* 2020; 20: 141-150.
- [16] Wang B, Jiang H, Zhou T, Ma N, Liu W, Wang Y and Zuo L. Expression of ICOSL is associated with decreased survival in invasive breast cancer. *PeerJ* 2019; 7: e6903.
- [17] Tang G, Qin Q, Zhang P, Wang G, Liu M, Ding Q, Qin Y and Shen Q. Reverse signaling using an inducible costimulator to enhance immunogenic function of dendritic cells. *Cell Mol Life Sci* 2009; 66: 3067-3080.
- [18] Tang Z, Li C, Kang B, Gao G, Li C and Zhang Z. GEPIA: a web server for cancer and normal gene expression profiling and interactive analyses. *Nucleic Acids Res* 2017; 45: W98-W102.
- [19] Ritchie ME, Phipson B, Wu D, Hu Y, Law CW, Shi W and Smyth GK. limma powers differential expression analyses for RNA-sequencing and microarray studies. *Nucleic Acids Res* 2015; 43: e47.
- [20] Yu G, Wang LG, Han Y and He QY. ClusterProfiler: an R package for comparing biological themes among gene clusters. *OMICS* 2012; 16: 284-287.
- [21] Newman AM, Liu CL, Green MR, Gentles AJ, Feng W, Xu Y, Hoang CD, Diehn M and Alizadeh AA. Robust enumeration of cell subsets from tissue expression profiles. *Nat Methods* 2015; 12: 453-457.
- [22] Szklarczyk D, Gable AL, Lyon D, Junge A, Wyder S, Huerta-Cepas J, Simonovic M, Doncheva NT, Morris JH, Bork P, Jensen LJ and Mering CV. STRING v11: protein-protein association networks with increased coverage, supporting functional discovery in genome-wide experimental datasets. *Nucleic Acids Res* 2019; 47: D607-D613.
- [23] Bader GD and Hogue CW. An automated method for finding molecular complexes in large protein interaction networks. *BMC Bioinformatics* 2003; 4: 2.
- [24] Shannon P, Markiel A, Ozier O, Baliga NS, Wang JT, Ramage D, Amin N, Schwikowski B and Ideker T. Cytoscape: a software environment for integrated models of biomolecular interaction networks. *Genome Res* 2003; 13: 2498-504.
- [25] Shan YS, Hsu HP, Lai MD, Yen MC, Chen WC, Fang JH, Weng TY and Chen YL. Argininosuccinate synthetase 1 suppression and arginine restriction inhibit cell migration in gastric cancer cell lines. *Sci Rep* 2015; 5: 9783.
- [26] Shan YS, Hsu HP, Lai MD, Yen MC, Fang JH, Weng TY and Chen YL. Suppression of mucin 2 promotes interleukin-6 secretion and tumor growth in an orthotopic immune-competent colon cancer animal model. *Oncol Rep* 2014; 32: 2335-42.
- [27] Martin-Orozco N, Li Y, Wang Y, Liu S, Hwu P, Liu YJ, Dong C and Radvanyi L. Melanoma cells express ICOS ligand to promote the activation and expansion of T-regulatory cells. *Cancer Res* 2010; 70: 9581-9590.
- [28] Shahi Thakuri P, Gupta M, Singh S, Joshi R, Glasgow E, Lekan A, Agarwal S, Luker GD and Tavana H. Phytochemicals inhibit migration of triple negative breast cancer cells by targeting kinase signaling. *BMC Cancer* 2020; 20: 4.
- [29] Bao H, Sin TK and Zhang G. Activin A induces leiomyoma cell proliferation, extracellular matrix (ECM) accumulation and myofibroblastic transformation of myometrial cells via p38 MAPK. *Biochem Biophys Res Commun* 2018; 504: 447-453.
- [30] Tang L and Han X. The urokinase plasminogen activator system in breast cancer invasion and metastasis. *Biomed Pharmacother* 2013; 67: 179-82.
- [31] Gomes LR, Terra LF, Wailemann RA, Labriola L and Sogayar MC. TGF- $\beta$ 1 modulates the homeostasis between MMPs and MMP inhibitors through p38 MAPK and ERK1/2 in highly invasive breast cancer cells. *BMC Cancer* 2012; 12: 26.
- [32] Wang B, Jiang H, Ma N and Wang Y. Phosphorylated-p38 mitogen-activated protein kinase

## ICOSL enhances tumor progression in TNBC

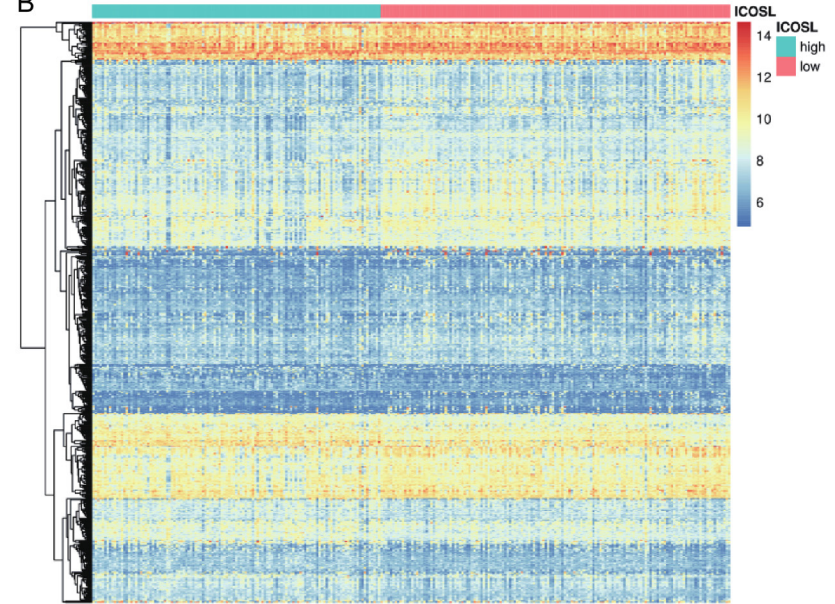
- expression is associated with clinical factors in invasive breast cancer. *Springerplus* 2016; 5: 934.
- [33] Narumi R, Murakami T, Kuga T, Adachi J, Shiromizu T, Muraoka S, Kume H, Kodera Y, Matsumoto M, Nakayama K, Miyamoto Y, Ishitobi M, Inaji H, Kato K and Tomonaga T. A strategy for large-scale phosphoproteomics and SRM-based validation of human breast cancer tissue samples. *J Proteome Res* 2012; 11: 5311-5322.
- [34] Yu K, Zhang Q, Liu Z, Zhao Q, Zhang X, Wang Y, Wang ZX, Jin Y, Li X, Liu ZX and Xu RH. qPhos: a database of protein phosphorylation dynamics in humans. *Nucleic Acids Res* 2019; 47: D451-D458.
- [35] Mertins P, Mani DR, Ruggles KV, Gillette MA, Clauser KR, Wang P, Wang X, Qiao JW, Cao S, Petralia F, Kawaler E, Mundt F, Krug K, Tu Z, Lei JT, Gatza ML, Wilkerson M, Perou CM, Yellapantula V, Huang KL, Lin C, McLellan MD, Yan P, Davies SR, Townsend RR, Skates SJ, Wang J, Zhang B, Kinsinger CR, Mesri M, Rodriguez H, Ding L, Paulovich AG, Fenyö D, Ellis MJ and Carr SA; NCI CPTAC. Proteogenomics connects somatic mutations to signalling in breast cancer. *Nature* 2016; 534: 55-62.
- [36] Amatore F, Gorvel L and Olive D. Inducible Co-Stimulator (ICOS) as a potential therapeutic target for anti-cancer therapy. *Expert Opin Ther Targets* 2018; 22: 343-351.
- [37] Wang B, Cheng H, Wang L, Zhou H and Wang J. Expression of ICOSLG on mouse hematologic neoplasm cell lines and their influence on cytotoxicity in allogeneic mixed lymphocyte reactions. *Leuk Lymphoma* 2012; 53: 674-80.
- [38] Faget J, Sisirak V, Blay JY, Caux C, Bendriss-Vermare N and Ménétrier-Caux C. ICOS is associated with poor prognosis in breast cancer as it promotes the amplification of immunosuppressive CD4 T cells by plasmacytoid dendritic cells. *Oncoimmunology* 2013; 2: e23185.
- [39] Mo L, Chen Q, Zhang X, Shi X, Wei L, Zheng D, Li H, Gao J, Li J and Hu Z. Depletion of regulatory T cells by anti-ICOS antibody enhances anti-tumor immunity of tumor cell vaccine in prostate cancer. *Vaccine* 2017; 35: 5932-5938.
- [40] Han Y, Dong Y, Yang Q, Xu W, Jiang S, Yu Z, Yu K and Zhang S. Acute myeloid leukemia cells express ICOS ligand to promote the expansion of regulatory T cells. *Front Immunol* 2018; 9: 2227.

# ICOSL enhances tumor progression in TNBC

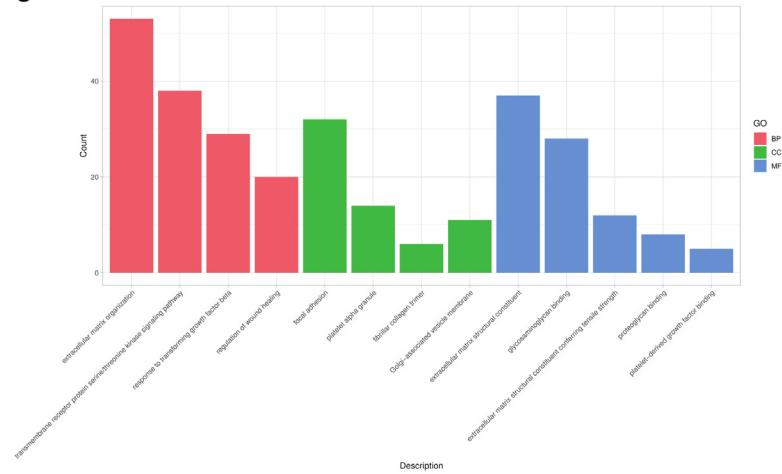
A



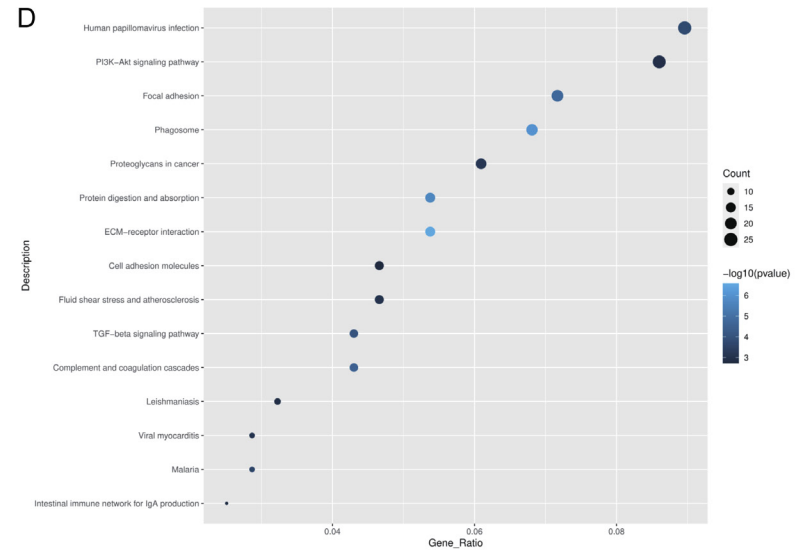
B



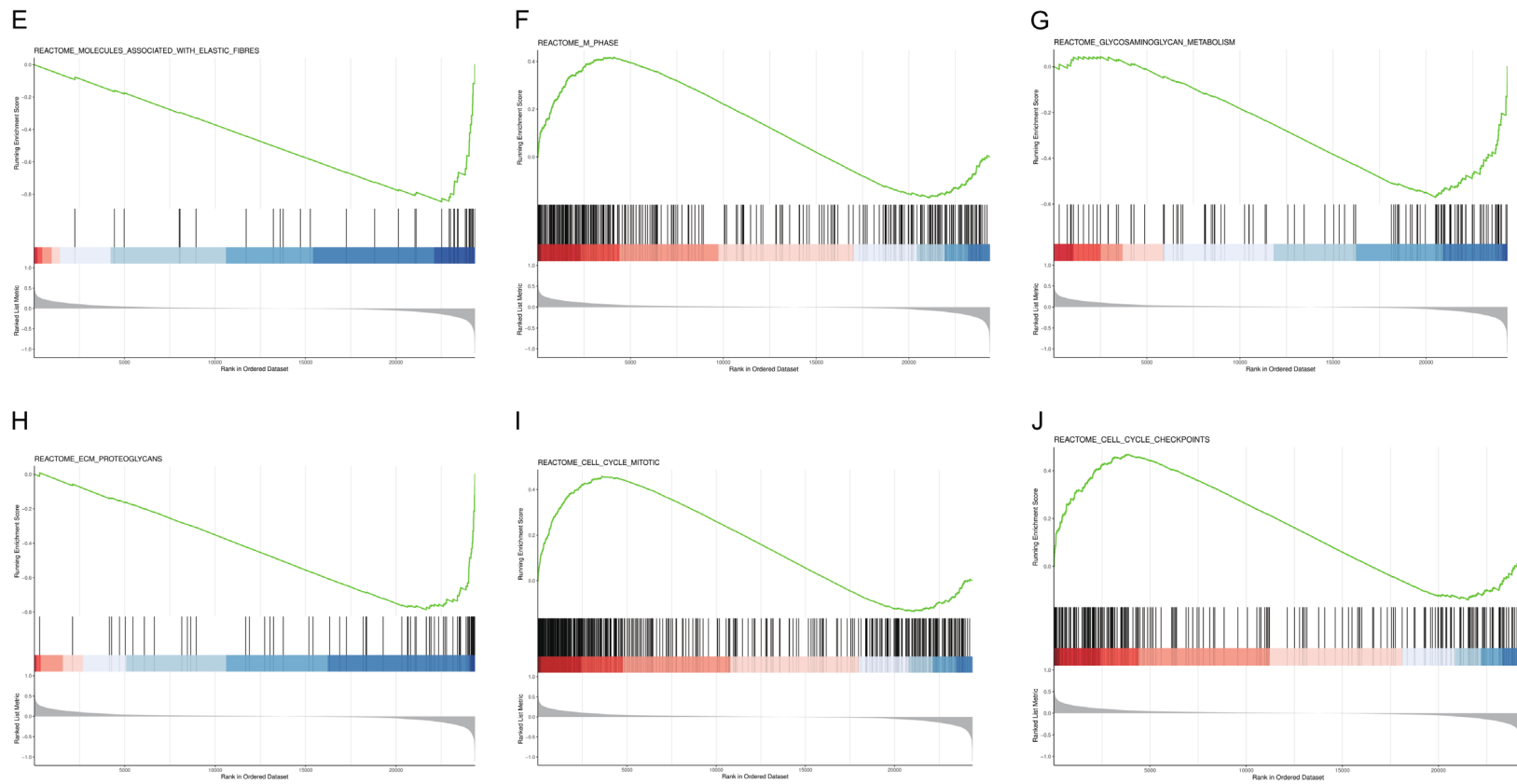
C



D



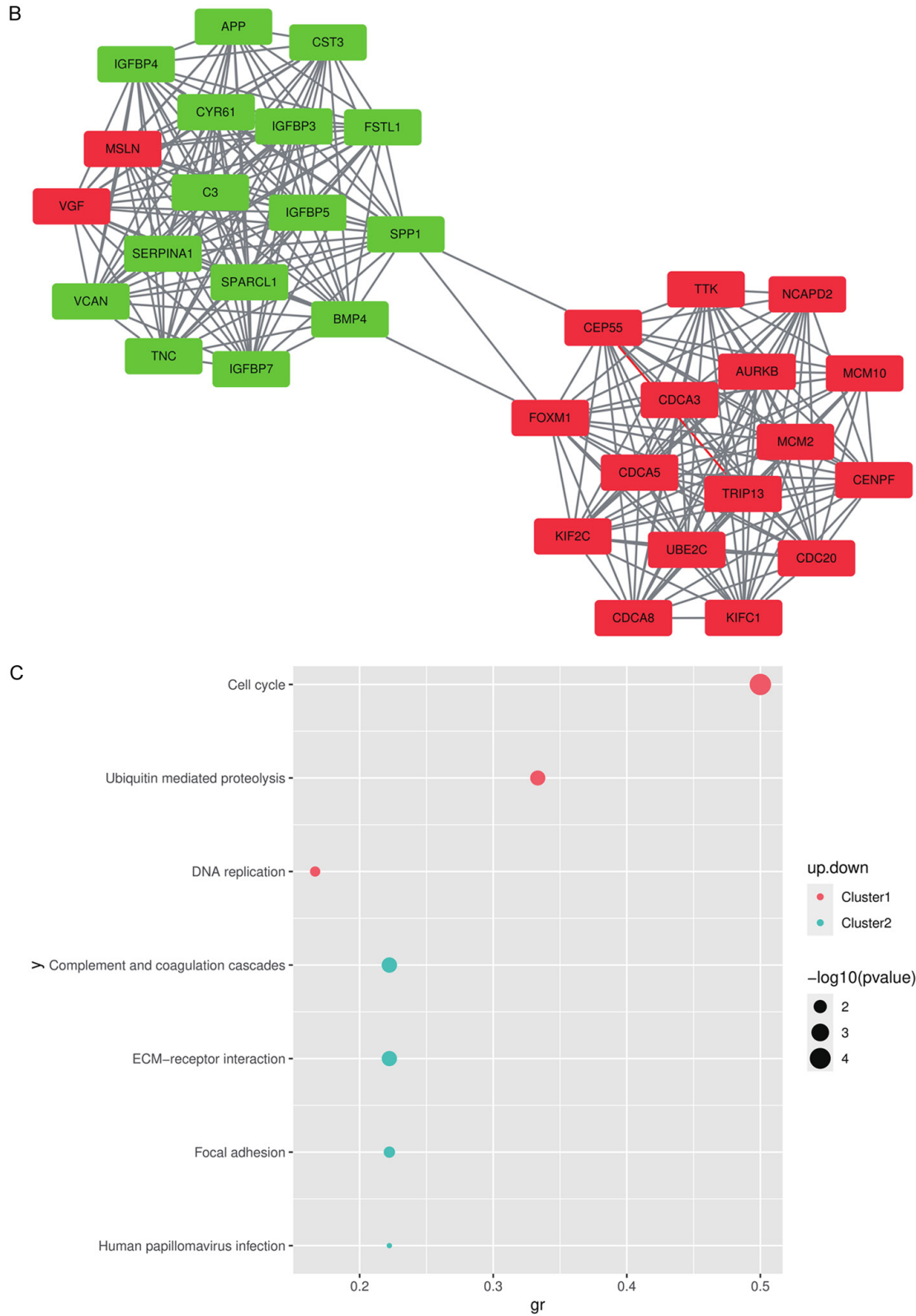
# ICOSL enhances tumor progression in TNBC



**Supplementary Figure 1.** DEGs, GO and KEGG analyses, and GSEA for ICOSL expression in the TNBC dataset. A. Volcano plot of differentially expressed genes. Red circles represent significantly upregulated genes, and blue circles represent significantly downregulated genes. B. Heatmap of differentially expressed genes. C. Gene ontology annotation of differentially expressed genes. D. KEGG pathway enrichment for differentially expressed genes. E-J. Reactome pathway enrichment via GSEA with REACTOME gene sets in msigdb.



# ICOSL enhances tumor progression in TNBC



**Supplementary Figure 2.** PPI network analysis of DEGs based on ICOSL expression in the TNBC dataset. A. PPI network for DEGs obtained from STRING online tools. B. MCODE cluster in the PPI network with the highest MCODE score. Red nodes indicate upregulated genes, and green nodes indicate downregulated genes. C. KEGG pathway enrichment for subclusters of the MOCDE cluster.